Supplemental Material — Measuring Topological Invariants from Generalized Edge States in Polaritonic Quasicrystals

Florent Baboux*[1], Eli Levy*[2,3], Aristide Lemaître[1], Carmen Gómez[1], Elisabeth Galopin[1], Luc Le Gratiet[1], Isabelle Sagnes[1], Alberto Amo[1], Jacqueline Bloch[1,4], Eric Akkermans[2]

*These authors contributed equally to this work.

[1]Centre de Nanosciences et de Nanotechnologies, CNRS, Univ. Paris-Sud, Université Paris-Saclay, C2N Marcoussis, 91460 Marcoussis, France

[2]Department of Physics, Technion Israel Institute of Technology, Haifa 32000, Israel

[3]Rafael Ltd., P.O. Box 2250, Haifa 32100, Israel and

[4]Physics Department, Ecole Polytechnique, Université Paris-Saclay, F-91128 Palaiseau Cedex, France

This Supplemental Material presents a derivation of the Fabry-Perot based geometrical model for the momentum-space and real-space properties of generalized edge states which is discussed in the main letter. We also discuss in the last section the occurrence of topologically trivial modes in our polaritonic quasicrystals.

FABRY-PEROT MODEL OF THE TOPOLOGICAL EDGE STATES

The effective Fabry-Perot model derived here is for a true 1D system, and is given in the language of the scattering theory, as originally proposed in Ref. [35]. The basic idea is to regard the interface between the Fibonacci sequences $\overleftarrow{F_N}(\phi)$ and $\overrightarrow{F_N}(\phi)$ as a virtual Fabry-Perot cavity, and correspondingly consider the chains $\overleftarrow{F_N}(\phi)$ and $\overrightarrow{F_N}(\phi)$ as mirrors. In this perspective, the generalized edge states localized at the interface between the two Fibonacci chains are interpreted as Fabry-Perot resonances (see Fig. 5).

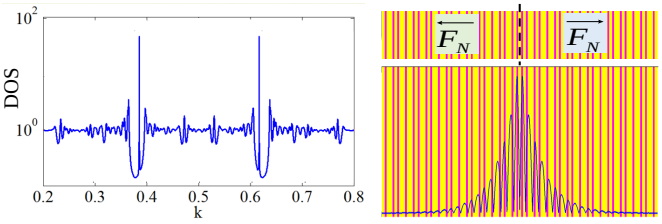

Figure 5. Appearance of gap states in the Fibonacci based structure $\overleftarrow{F_N}\overrightarrow{F_N}$ with $N = 55$. (a) Density of states spectrum DOS(k) with interface states appearing in the gaps (here at normalized wavevectors $k = 0.39$ and $k = 0.61$). (b) Spatial arrangement of the structure $\overleftarrow{F_N}\overrightarrow{F_N}$ indicated by yellow and magenta bars (corresponding to letters A and B), with a representation of the spatial profile of the gap state at $k = 0.39$.

Qualitatively speaking, the Fibonacci chains $\overleftarrow{F_N}(\phi)$ or $\overrightarrow{F_N}(\phi)$ which have a gapped spectrum are mirrors for specific frequencies, due to the high reflectance values at the spectral gaps. These mirrors are not standard, since they provide a frequency-dependent phase shift upon reflection due to multiple reflections. This phase shift, as we will show now, allows to treat an interface between two such structures as a virtual (not geometric) cavity length.

The standard Fabry-Perot resonance condition for a cavity of length L, given by

$$2L/\lambda_m = m, \quad m \in \mathbb{Z}, \tag{1}$$

($\{\lambda_m\}$ being a discrete set of resonant wavelengths), is a basic constructive interference condition. Therefore, it may always be written in terms of the winding of a phase: the cavity phase θ_{cav}, representing the total round-trip phase inside the cavity and defined by

$$\theta_{\text{cav}}(k, L) \equiv \frac{4\pi L}{\lambda(k)}, \tag{2}$$

where $\lambda(k) = 2\pi/k$ is the wavelength. This gives a resonance condition equivalent to Eq. (1), namely

$$\theta_{\text{cav}}(k_m) = 2\pi m \ , \ m \in \mathbb{Z}. \tag{3}$$

Here we follow the very same argument, but in the reverse order. We begin with the structure $\overrightarrow{F_N}\overleftarrow{F_N}$, which is a cavity of zero (geometrical) length. The cavity phase is however non-zero, as $\overleftarrow{F_N}$ and $\overrightarrow{F_N}$ both yield a non-zero phase upon reflection. If we define the reflected phase shift for the left boundary of $\overrightarrow{F_N}$ as $\overrightarrow{\theta}_{\text{left}}(k)$, then the cavity phase for $\overrightarrow{F_N}\overleftarrow{F_N}$ is $2\overrightarrow{\theta}_{\text{left}}(k)$. Now, similarly to Eq. (2), a virtual cavity length is defined as

$$\mathcal{L}(k, \theta_{\text{cav}}) \equiv \frac{\lambda(k)}{4\pi}\theta_{\text{cav}}, \tag{4}$$

with resonant interface states occurring at gap frequencies satisfying the Fabry-Perot condition

$$2\mathcal{L}(k_m)/\lambda(k_m) = m, \quad m \in \mathbb{Z}. \tag{5}$$

The model then predicts that for every value of $\lambda(k_m)$ lying within a spectral gap, a new interface state will exist.

This reasoning is utilized in Eqs. (2) and (3) of the main letter directly through θ_{cav}, to define the topological winding number of the generalized edge state when the phason ϕ is scanned. In that case, the scanning of ϕ monotonically drives the cavity phase (at gap frequencies) such that the resonant states monotonically change

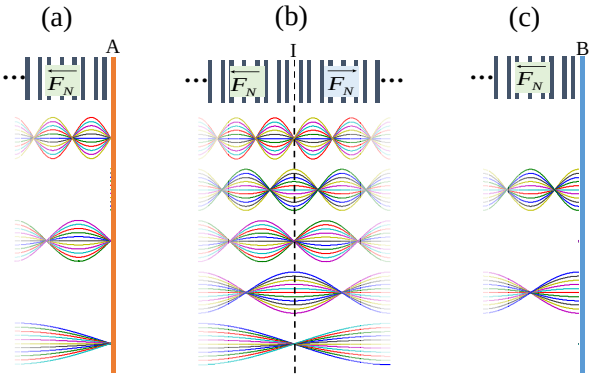

Figure 6. Different boundary conditions for the Fibonacci chain. (a) and (c): The Fibonacci chain $\overleftarrow{F_N}$ with $N = 55$ bounded from the right (a) by a metallic mirror (orange line), or (c) by a continuum with refractive index smaller than that of the chain (blue line). The presence of a node or antinode of the gap states at the boundary is here rigidly imposed by the boundary conditions. (b) The unfolded structure $\overleftarrow{F_N}\overrightarrow{F_N}$, based on the same structure, hosts generalized edge states which can possess either a node or an antinode at the interface (dotted line).

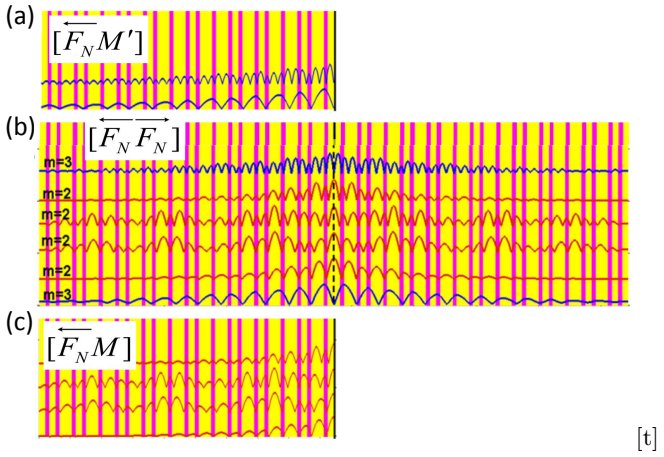

[t]

Figure 7. Real space profile of selected gap states for the structures depicted in Fig. 6: (a) The $\overleftarrow{F_N}$ chain with metallic reflective boundary, (b) the unfolded structure $\overleftarrow{F_N}\overrightarrow{F_N}$ and (c) the $\overleftarrow{F_N}$ chain with a refractive-index mismatch boundary.

frequency with ϕ. This reasoning fully supports the experimental observation of the topological winding of generalized edge states as a function of ϕ in momentum space, as evidenced in Fig. 3a,b of the letter. We now describe a Fabry-Perot property in real space that helps to further clarify the interplay between the topological and the Fabry-Perot properties of the generalized edge states.

The structure $\overleftarrow{F_N}\overrightarrow{F_N}$ is described in the main letter as a host for generalized edge states, in contrast to previous studies considering the interface with the vacuum. To clarify this, we consider the $\overleftarrow{F_N}$ chain bounded from the right by a perfect mirror. Waves traveling through the structure and towards the mirror plane are reflected back into the chain, experiencing the quasiperiodic modulation in the reverse order ($\overrightarrow{F_N}$). An equivalent version of this setup consists in removing the mirror and unfolding the chain with respect to the mirror plane, resulting in the structure considered in the main letter. The equivalence between these two boundary conditions is however not total. In particular, the structure $\overleftarrow{F_N}\overrightarrow{F_N}$ may host interface states which are both spatially symmetric and anti-symmetric with respect to the interface, namely with a node or an anti-node at the interface, as seen in Fig. 6b. In contrast to that, a single $\overleftarrow{F_N}$ chain bounded by a perfect mirror can host only one type of states: with a node on the mirror in the case of a metallic mirror, as shown in Fig. 6a, or with an antinode in the case of a mismatched mirror (continuum with refractive index smaller than that of the chain), as shown in Fig. 6c.

The fact that the generalized-edge scheme allows all possible interface states yields an additional degree of freedom to probe the topological content of the states. Indeed, topological information may be extracted from the real space properties of the edge states through the parity of the Fabry-Perot integer, m in Eq. (5). In the usual Fabry-Perot picture for phase-conserving perfect mirrors, odd and even values of m alternate between anti-symmetric and symmetric states with respect to the mid-cavity coordinate (with a node and an antinode at mid-cavity) respectively. This result is also true for our Fabry-Perot cavity with a ϕ dependent virtual length. This leads to two possible predictions.

Firstly, for a given value of ϕ, edge states residing in the various gaps have different spatial symmetries completely predictable by the Fabry-Perot model through the parity of m. For instance, Fig. 7 shows that modes with $m = 2$ (red) are symmetric with respect to the interface, while modes with $m = 3$ (blue) are antisymmetric. Again, we here see that the general-edge scheme (7b) hosts the union of all edge states of the metallic and index-mismatched boundary conditions (7a,c) taken together.

Secondly, for a given gap, generalized edge states traverse the gaps as a function of ϕ due to a monotonic change in the cavity phase. This means that when an edge state merges with one band-edge and a new state bifurcates from the other band-edge, then the parity of m flips and so does the spatial symmetry of the edge state. This is the theoretical argument supporting the experimental observation reported in Fig. 4 of the main letter. These features demonstrate that the use of generalized edges yields an additional degree of freedom (the symmetry index) that can be used to directly measure the topological invariants of the quasicrystal.

TOPOLOGICALLY TRIVIAL MODES OF THE POLARITONIC QUASICRYSTALS

In this section we show that our polaritonic structures also hosts topologically trivial modes, that can be clearly distinguished from the topological modes described above. An example is given in Fig. 2a,b of the main letter.

Among the states that are localized at the interface between the $\overleftarrow{F_N}$ and $\overrightarrow{F_N}$ sequences, one of them (at energy ~ 1596.5 meV) lies below the bulk band structure and is thus topologically trivial.

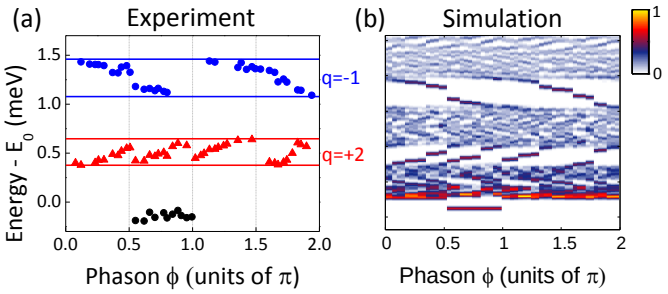

Figure 8. (a) Measured energy of the interface states (for the structure considered in Figs. 2,3,4 of the main letter) as a function of the phason ϕ. The topologically trivial mode is indicated with black circles. E_0 denotes the energy of the lowest bulk mode, and the solid lines indicate the gap boundaries. (b) Calculation of the whole energy spectrum from the 2D Schrödinger equation, as a function of ϕ.

This mode only appears for a particular quadrant of ϕ (between $\pi/2$ and π), for which the sequence of letters at the interface is AAAA. Since in our samples, the letter A corresponds to a lower potential value, this AAAA sequence forms a spatially extended potential well, and the mode that is seen is a bound mode of this well. To verify that this mode is topologically trivial, we can monitor its spectral evolution as a function of ϕ, both in the experiment and the simulation (2D Schrödinger calculation) as shown in Fig. 8. We observe that the mode only appears in the quadrant $[\pi/2, \pi]$ and keeps a constant energy within the experimental error: it does not perform any spectral traverse as the phason is scanned, which confirms its topologically trivial nature.